SIPredict: Efficient Post-layout Waveform Prediction via System Identification

Qicheng Huang[1], Xiao Li[1], Fan Yang[1*], Xuan Zeng[1*], and Xin Li[1,2]
[1]State Key Lab of ASIC & System, Microelectronics Dept., Fudan University, Shanghai, P. R. China
[2]Electrical and Computer Engineering, Carnegie Mellon University, Pittsburgh, PA, U.S.A.

Abstract— In this paper, we propose a post-layout waveform prediction method by System Identification (SI) based on the fact that the waveforms of pre-layout and post-layout are always correlated. Mathematical models are built to describe the relationships between the pre-layout and post-layout simulation results via SI techniques. The model parameters are calibrated by using the simulation results of the first few data points of pre-layout and post-layout stages. By taking the corresponding pre-layout simulation results as inputs of the calibrated models, the rest post-layout waveforms can thus be predicted as the output of the models. Several examples demonstrate the efficiency of the prediction, which helps the designers have a quick view of the post-layout waveforms in the design process.

I. Introduction

Post-layout simulation is important but computation-intensive in Analog Mixed-Signal (AMS) circuit design. After parasitic extraction, the number of nodes and elements of the AMS circuits increase 10x compared with the pre-layout ones. The post-layout simulation of AMS circuits would thus take a long period. It is crucial to develop efficient methods to obtain the post-layout simulation waveforms.

Model Order Reduction (MOR) is considered as the most powerful approach to address the post-layout simulation problem [1–4]. MOR techniques produce reduced-order models for the interconnects and thus reduce the computational cost for post-layout simulations. A variety of MOR methods have been developed in the past decades, among which the elimination based methods such as PACT [1] and TICER [2] have been successfully applied to the post-layout simulation of AMS circuits.

The pre-layout and post-layout simulation data come from the same circuit. Therefore, they are expected to be strongly correlated. It is possible to utilize the information from the pre-layout simulation to accelerate the post-layout analysis. Recently, Bayesian Model Fusion (BMF) has been developed to employ the early stage simulation data to accelerate the parametric yield analysis in the late stage [5]. With the early stage data, BMF methods can greatly reduce the number of late-stage samples for parametric yield analysis. On the other hand, Transient analysis is one of the most critical tasks in AMS circuit design and verification flow. The transient simulation results can help the designers to diagnose and optimize the circuits. For an AMS circuit, the transient simulation waveforms of the pre-layout and post-layout stages are also strongly correlated. Therefore, it is possible to predict the post-layout waveforms from the pre-layout simulation results. However, this problem has not been studied before.

System identification methods [6] have been well developed to build mathematical models of dynamic systems based on the observed data, and have been successfully applied to many areas, such as industrial process [7], automatic control [8] and neural networks [9]. In this paper, we propose a post-layout waveform prediction method via system identification. System models are used to describe the correlations between the post-layout and pre-layout waveforms. We treat the waveforms of pre-layout and post-layout stages as the inputs and outputs of the systems, respectively. The systems are calibrated via system identification by using the simulation results of the first few data points of pre-layout and post-layout stages. By taking the corresponding pre-layout simulation results as inputs of the calibrated models, the rest post-layout waveforms can thus be predicted from the outputs. In this way, we can quickly predict the waveforms of the critical nodes by only simulating the post-layout circuits for a short period. The proposed technique is very helpful for the AMS designers to quickly explore the waveforms of the critical nodes of post-layout circuits without expensive circuit simulation.

The remainder of this paper is organized as follows. In Section 2, we will introduce the background and motivation of our work. The proposed post-layout waveform prediction method via system identification will be presented in Section 3. The efficiency of the proposed method is demonstrated by several examples in Section 4. Finally, We conclude the paper in Section 5.

II. Background and Motivation

In the AMS circuit design and verification process, designs would be optimized and verified for several times before finalization. The parasitic resistors and capacitors could greatly affect the performance of the designs. Thus, it is necessary to take the parasitics into consideration even in the design stages. However, the post-layout simulation is time-consuming and usually it is impossible to run post-layout simulations during the design stages. During the design stages, designers just want to know how the circuit performances are affected by the parasitics, which can guide them to diagnose and optimize the designs. Therefore, an prediction method that can predict the post-layout waveforms efficiently, would be very helpful for designers.

*Corresponding authors. Email: {xzeng, yangfan}@fudan.edu.cn.

978-1-4799-7792-5/15/$31.00 ©2015 IEEE

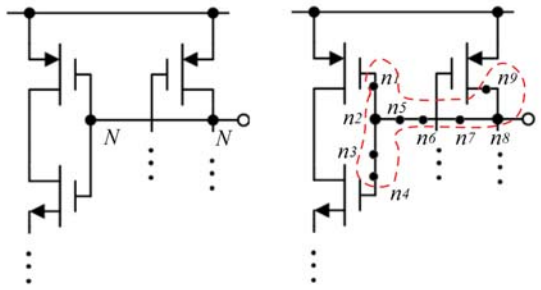

Fig. 1. Part of a sense amplifier circuit. The node N of pre-layout stage on the left corresponds to nodes $n1 \cdots n9$ of post-layout stage on the right.

The post-layout circuits are generated from the pre-layout circuits by adding the parasitic resistors, capacitors and inductors. Take part of a sense amplifier circuit as an example. Fig. 1 shows part of the pre-layout and post-layout circuits of a sense amplifier. In the left sub-figure, the MOSFETs are connected directly in the pre-layout circuit. But for the post-layout circuit shown in the right sub-figure, the MOSFETs are connected through interconnects modeled by complex RLC sub-circuits. Several new nodes such as $n1$, $n3$, $n5$ are added in the post-layout circuit to replace the single node N in the pre-layout circuit.

Node N in the pre-layout circuit corresponds to nodes $n1 \cdots n9$ in the post-layout circuit. The waveforms of nodes $n1 \cdots n9$ are similar but not identical to node N because the existence of parasitic elements. The strong correlations inspired us to utilize the simulation data of pre-layout circuits to predict the post-layout waveforms.

By the complete pre-layout simulation and a limited time period of post-layout simulation, we can predict the rest post-layout waveforms. This means that we are able to quickly explore the post-layout waveforms without time-consuming simulation. On the other hand, we should point out that due to the use of system identification instead of solving circuit equation, the predicted responses may not always be accurate and thus the prediction method cannot be used for sign-off. However, the predicted waveforms can provide the designers with guidance for further optimization. Several examples have demonstrated that compared with the pre-layout waveforms, the predicted ones are far more similar to the post-layout waveforms, and some even with high accuracy.

III. The Proposed SIPredict Method

In this section, we will present the proposed post-layout waveform prediction method via system identification (SIPredict).

A. Syetem Models

System models are used to describe the correlations of the pre-layout and post-layout waveforms. The pre-layout and post-layout waveforms are taken as the inputs and outputs of the systems, respectively. We will present the system models used in our prediction method in this subsection.

The black-box system models are chosen for our SIPredict method, which means we assume that the system is unknown and all parameters are adjustable without consideration of the physical meanings. A variety of models including three linear and two non-linear models are introduced in this paper. For an AMS circuit, the waveforms of the post-layout simulations would not change greatly compared with the pre-layout simulation results. Therefore, a linear model is often sufficient to accurately describe the correlation between the pre-layout and post-layout simulation results. In most cases, we will try to fit linear models first. For the scenarios that the linear models provide poor fits or the correlation exhibits significant nonlinearity, we will use the nonlinear models.

The linear candidate models include ARX model, impulse-response model and transfer function model. The nonlinear candidate models include nonlinear ARX model and Hammerstein-Wiener model. We will introduce these models in the rest of this subsection. After the candidate models are calibrated and validated, the model with the highest fit-level for the validation data is selected to predict the post-layout waveforms.

A.1 Impulse-response Model

It is well known that for a linear, time-invariant, casual system, the output response to a general input $u(t)$ can be described as the convolution with the impulse response. In the continuous-time domain, we have

$$y(t) = \int_{\tau=0}^{t} g(\tau)u(t-\tau)d\tau, \tag{1}$$

where the impulse response $g(t)$ is the output of the system with the impulse signal as input.

In discrete-time domain, we have

$$y(k) = \sum_{n=0}^{k} g(n)u(k-n), \tag{2}$$

where $g(k)$ is the discrete time impulse response.

The convolution model fully characterized by the impulse response function $g(k)$, is able to describe the input-output relationship of LTI systems. Once $g(k)$ is known, the corresponding output can be easily computed for a given input $u(k)$. This feature explains the interests in impulse response model representations especially when the prior knowledge about system behavior is limited [10]. Impulse response model is one of the simplest linear models, for it has no memory and the output is only dependent on the input, which exhibits a static behavior.

A.2 ARX Model

ARX (Auto-Regressive eXogenous) model [6] is a special case of the general linear polynomial model. It can be described by

$$A(q)y(k) = B(q)u(k) + e(k), \tag{3}$$

where

$$\begin{aligned} A(q) &= 1 + a_1 q^{-1} + \cdots + a_{n_a} q^{-n_a}, \\ B(q) &= b_1 q^{-1} + \cdots + b_{n_b} q^{-n_b}, \end{aligned}$$

$e(k)$ denotes the measurement noise sequence. Since the data are obtained via simulation rather than physical measurement, we can simply ignore $e(k)$. q is a delay operator. For a signal $u(k)$ in time domain, $q^{-1}u(k)$ means $u(k-1)$ here. An equivalent model of (3) can also be expressed as

$$y(k) + a_1 y(k-1) + \cdots + a_{n_a} y(k-n_a) = b_1 u(k-1) + \cdots + b_{n_b} u(k-n_b). \quad (4)$$

Generally ARX model is denoted as $ARX(n_a, n_b, n_k)$, where n_a and n_b denote the orders of $A(q)$ and $B(q)$ polynomials respectively and n_k indicates the number of sampling intervals related to dead time(input-output delay). Consequently, in case of dead time, $b_1 = \cdots = b_{n_k} = 0$ [10].

Compared to impulse response model, ARX model is a more complex dynamic model since its output depends on not only the inputs but also the history states. In the special case $n_a = 0$, ARX model is reduced to the impulse response model.

A.3 Transfer Function Model

Laplace transformation is one of the basic tools in linear system analysis. In Laplace domain, the transfer function of a system can be generally written as

$$Y(s) = \frac{num(s)}{den(s)} U(s) + E(s), \quad (5)$$

where $Y(s)$, $U(s)$ and $E(s)$ represent the Laplace transforms of the output, input and noise respectively. Similarly, we ignore the noise term $E(s)$ here. $num(s)$ and $den(s)$ represent the numerator and denominator polynomials that define the relationship between input and output. The roots of the denominator and the numerator polynomials are referred to as the poles and zeros of models respectively.

A.4 Nonlinear ARX Model

In linear ARX model (4), the current output $y(k)$ is predicted by a linear combination of the regressors $y(k-1)\cdots y(k-n_a)$, $u(k-1)\cdots u(k-n_b)$. Nonlinear ARX model [11] extends the linear formula to a nonlinear mapping function as:

$$y(k) = f(y(k-1), \cdots y(k-n_a), u(k-1), \cdots u(k-n_b)). \quad (6)$$

The nonlinear function f is a combination of a linearity estimator and a nonlinearity estimator. The linearity estimator has the same form as (4), while the nonlinearity estimator is a sum of series of nonlinear elements, such as wavelet networks or sigmoid functions. Nonlinear ARX model is an extension and supplement for linear models when they are not sufficient to accurately describe the system dynamics.

A.5 Hammerstein-Wiener Model

Hammerstein-Wiener model [6] is one of the most commonly used nonlinear models with static nonlinearities both at the inputs and outputs.

Fig. 2 shows a block diagram of Hammerstein-Wiener model, where

$$w(k) = f(u(k)), x(k) = (B(q)/F(q))w(k), y(k) = h(x(k)).$$

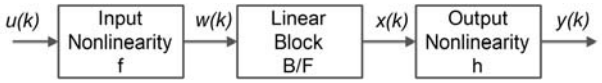

Fig. 2. A block diagram represents the structure of Hammerstein-Wiener model.

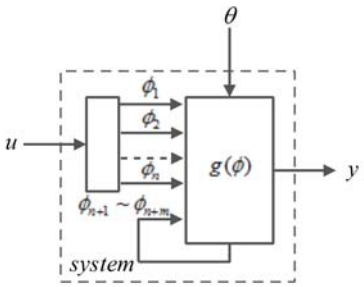

Fig. 3. A general model to describe the system models.

Here f is a nonlinear function which maps input data $u(k)$ to the internal linear system. $B(q)/F(q)$ is a linear transfer function that represent the internal linear system, and h is a nonlinear function that maps the output of the internal linear system to the external output.

B. Model Calibration

The parameters of the system models are determined in the model calibration procedure. We run the post-layout simulations for a short time and combine the simulation results together with the corresponding pre-layout simulation results for calibration. The parameters are derived by minimizing the error of the response predicted by the system models and the real waveform. For some specific circuits, the waveforms of transient stages should not be used for model calibration, because the correlation of pre-layout and post-layout waveforms can be barely reflected in the transient stages. In this case, we have to prolong the simulation and start to collect the simulation data after the circuits work properly.

For linear system models, we use a general model as shown in Fig. 3 to describe the system models presented in the previous subsection. In this general model, the system is the function of the system inputs and the past system outputs. The task of the calibration procedure is to find the expression of the function $g(\phi)$, which is parameterized by a set of parameters θ [6] as:

$$g(\phi) = \theta_1\phi_1 + \theta_2\phi_2 + \cdots + \theta_{n+m}\phi_{n+m},$$

where

$$\phi = \left[\ \phi_1 \cdots \phi_{n+m}\ \right]^T,$$
$$\left[\ \phi_1 \cdots \phi_n\ \right]^T = \left[\ u(k-1) \cdots u(k-n)\ \right]^T,$$
$$\left[\ \phi_{n+1} \cdots \phi_{n+m}\ \right]^T = \left[\ -y(k-1) \cdots -y(k-m)\ \right]^T.$$

The goal of model calibration is to find the optimal parameters $\vec{\theta_c} = \{\ \theta_{c_1}, \cdots, \theta_{c_{n+m}}\}$ that minimize the error of the output $\tilde{y}$ predicted by the model over the first few time points $\{0, \cdots, s\}$:

$$\vec{\theta_c} = argmin V_N(\theta), \quad (7)$$

where

$$V_N(\theta) = \frac{1}{N}\sum_{i=1}^{s}[y(i) - \tilde{y}(i)]^2,$$

and this can be easily solved using ordinary least squares estimation.

Also, for a certain type of linear model, the orders of the models should be determined before the model calibration process. For example, we should determine n_a and n_b in the ARX model before the model calibration. In our implementation, besides using prior knowledge about the AMS circuits, we determine a general range of orders according to [10], and then select the orders that predict the responses in highest accuracy.

Similarly, for nonlinear ARX model and the Hammerstein-Wiener model, we use iterative search to minimize the simulation error between the model output and the measured output. Due to the limited space, please refer to [6] and [12] for the details of the calibration procedure.

C. Model Validation

The minimization of prediction error in model calibration procedure cannot always lead to accurate models. So after the system models are calibrated, we further use a set of new post-layout simulation data to validate them.

We first define a fit-level function (%) [13] to judge the accuracy of the calibrated models as below

$$fit\_level = 100\left(1 - \frac{||y - \tilde{y}||}{||y - mean(y)||}\right),$$

where y is the measured data and $\tilde{y}$ is the output of the calibrated model. $mean(y)$ denotes the mean value of the measured data over all the time points. The fit-level (%) is the mean square error between the measured data and the simulated output of the model. 100% fit-level corresponds to a perfect fit (no error) and 0% fit-level corresponds to a bad fit.

We will choose the best models in the candidate models according to their fit-levels for the validation data to predict the remaining post-layout waveforms.

D. Algorithm Summary

We summarize the proposed algorithm SIPredict in Fig. 4. In the proposed algorithm, the corresponding pre-layout nodes of the interested post-layout nodes are extracted firstly. Then, the post-layout circuit is simulated for a short time period. Part of the result is taken as calibration data and the rest is taken as validation data. Afterwards, the calibration data and the corresponding data points of the pre-layout simulation are employed to calibrate the parameters of system models. Finally the model with highest fit-level for validation data is selected. If its fit-level is acceptable, we use it for the prediction of the remaining post-layout waveform.

In our proposed method, we first try all the linear system models presented in section 3.A. If the fit-level is lower than a threshold, we will try the more complex nonlinear system models. If the fit-level of the nonlinear system model is still unacceptable, a post-layout simulation should be performed to derive the waveforms.

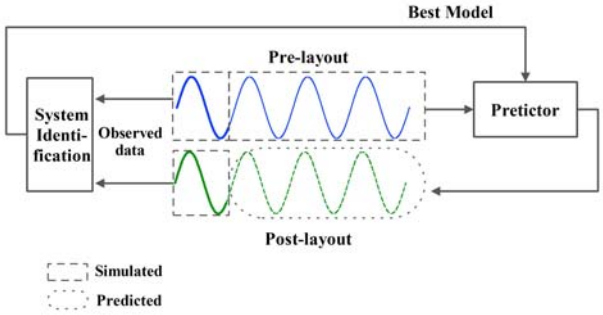

Fig. 4. SIPredict algorithm flow.

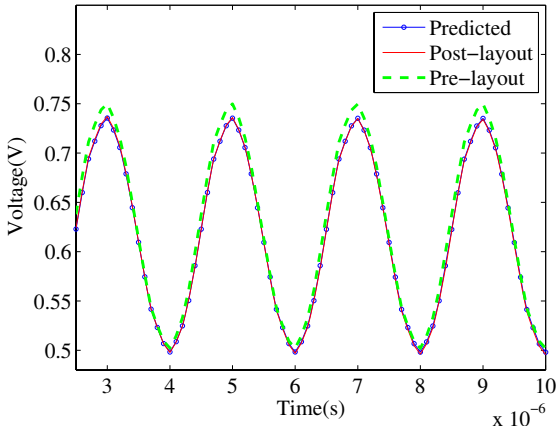

Fig. 5. The predicted, the pre-layout and post-layout waveforms of the output node of the operational amplifier.

IV. Experimental Results

In this section, four circuit examples are used to demonstrate the efficiency of our proposed SIPredict method. Linear models are accurate enough for prediction of the first two examples, but they offer poor fit-levels for the last two more complicated examples. As a result, we use more complex and flexible nonlinear models to predict the waveforms of the last two examples. All experiments are run on a PC with Intel 2.50GHz CPU and 4GB memory.

From our experiments, we can find that the waveforms predicted by our proposed method cannot always achieve very high accuracy. However, the predicted waveforms can essentially predict the trends of the waveforms, which can guide the designers to diagnose and optimize their designs.

A. Operational Amplifier

In this example, the test circuit is a folded cascade operational amplifier (op-amp) designed in a 32nm CMOS process. The pre-layout and post-layout waveforms of the output node are depicted in Fig. 5, which shows that the discrepancy is mainly the amplitude attenuation.

The whole simulation waveforms contain 1000 data points. Because the output waveform is obvious periodic, we choose the first 200 data samples containing a complete waveform period to calculate the parameters. We picked the next 50 samples for model validation.

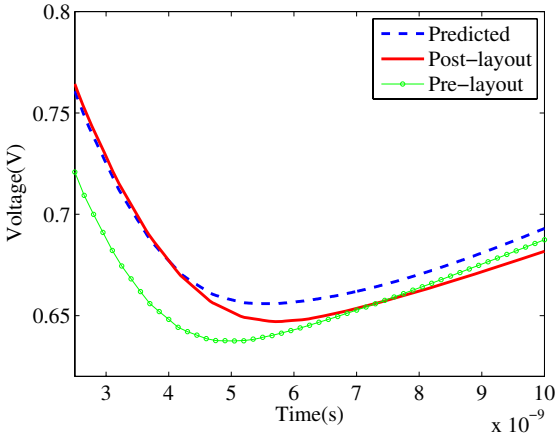

Fig. 6. The predicted, the pre-layout and post-layout waveforms of node BL of the sense amplifier

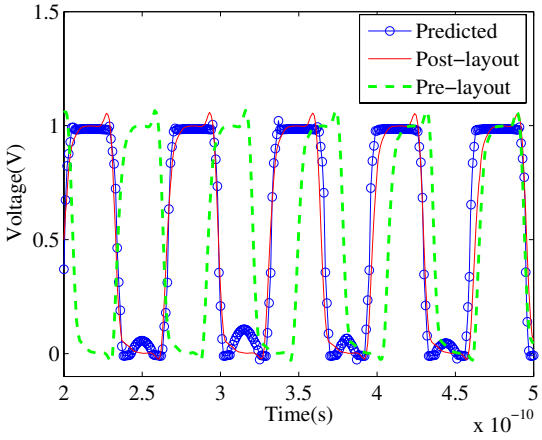

Fig. 7. The predicted, the pre-layout and post-layout waveforms of the output of the ring oscillator.

Table I shows the fit-level and the runtime of model calibration and model validation of the three candidate linear models. Since ARX model achieves the highest fit-level, we use it to predict the final waveform with fit-level of 98.43%. Thus we achieved a nearly 100% accuracy by using the first $1/4$ data. The predicted waveform is also shown in Fig. 5, from which we can see the predicted waveform is nearly identical to the post-layout waveform while there is obvious amplitude difference from the pre-layout waveform.

B. Sense Amplifier

Sense amplifier is an important component to perform the read operation for static random-access memory (SRAM). We use the simplified circuit of a latch-based sense amplifier designed in a 32nm CMOS process in this experiment. Its differential outputs (BL and BL_) are connected to two bit lines of an SRAM. After a small voltage difference is imposed to BL and BL_, the waveform of BL first goes down and then gradually climbs to high level.

The whole simulation waveforms contain 1000 data points. We choose the first 250 data points of pre-layout and post-layout waveform for prediction, with the first 150 data points for model calibration and the rest 100 data points for model validation. Since transfer function model achieves the highest fit-level, we use it to be the best approximate of the system and it predicts the final waveform with fit-level of 93.4%. Fig. 6 also shows the predicted waveform of node BL, which is nearly identical at first and keep almost the same slope afterwards. The pre-layout waveform, on the other hand, is quite different from the post-layout waveform. By using the first $1/4$ data, we successfully predict the trend and shape of the post-layout waveform.

C. Ring Oscillator

In this case, we use a ring oscillator which consists of several inverters in series to show the efficiency of the nonlinear models. The pre-layout and post-layout waveforms of the output of the ring oscillator are depicted in Fig. 7. The discrepancy is much more complex, since it is not a simple time delay but acts as the period prolongation. Therefore, the linear models are not able to describe the complex correlations any more. We use Hammerstein-Wiener model for prediction in this example because the nonlinearity in the input and output blocks should be suitable to represent the period prolongation.

The whole simulation waveforms contain 500 data points. Although the input and output are also periodic signals, we cannot choose only one period of data as the operation amplifier example. Because the main difference of pre-stage and post-stage is period prolongation rather than amplitude attenuation and more than one period data is essential for defining the period difference. We choose the first 150 data, which comprise about three periods of pre-layout and post-layout waveforms, for model calibration. The next 50 data samples are picked for model validation. In the validation process, Hammerstein-Wiener model achieves a fit-level of 91.07%, so it is qualified to describe the system and finally it predicts the final waveform with fit-level of 78.95%. Fig. 7 shows the predicted waveform of the output node, from which we can see the period prolongation is accurately predicted, although there are some detail errors in amplitude.

D. Phase Locked Loop

In this example, we use a much more complicated circuit: Phase Locked Loop (PLL). The waveform of the "locked" signal is critical to a PLL design. The pre-layout and post-layout waveforms of the "locked" signal are depicted in Fig. 8, from which we can see the locking time and final voltage is quite different, and the discrepancies appear as both time delay and amplitude difference.

In this case, nonlinear ARX model is used to describe the complex correlation between the waveforms. The whole waveforms contain 5000 data points. We drop the first 500 points because the PLL is still initializing at these points. We choose the following 800 data samples for model calibration. The next 500 data samples are picked for model validation. Finally the nonlinear ARX model achieves a fit-level of 89.85% for the validation data, and it predicts the remaining waveform with fit-level of 73.5%. Fig. 8 shows the predicted waveform of the output node, from which we can see it is much more similar to

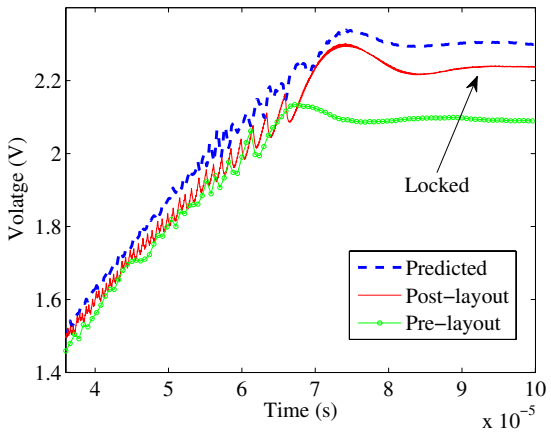

Fig. 8. The predicted, the pre-layout and post-layout waveforms of the output of the PLL.

TABLE I
LINEAR MODEL PREDICTION INFORMATION OF SENSE AMPLIFIER AND OPERATIONAL AMPLIFIER

Circuits	Model type	Fit-level of validation (%)	Fit-level of prediction (%)	Model calibration time(s)	Prediction time (s)
op-amp	ARX[a]	98.79	98.43	0.202	0.042
	TF[b]	95.07	93.46	3.162	0.035
	IMP[c]	94.73	94.75	0.292	0.041
sense-amp	ARX	97.63	87.38	0.423	0.058
	TF	99.57	93.50	4.819	0.053
	IMP	94.59	84.71	0.683	0.035

[a] ARX Model
[b] Transfer Function Model
[c] Impulse Response Model

the post-layout waveform and the indicated lock time is almost the same.

The post-layout simulation of PLL takes 1853.4 seconds. However, the SIPredict method uses only several seconds to predict the desired waveform. Although the actual post-layout simulation time may vary for different circuits, the corresponding prediction time by the proposed SIPredict method is nearly constant. As a result, the proposed method can effectively reduce the post-layout analysis time.

V. CONCLUSION

In this paper, we propose a method for post-layout waveform prediction via system identification. We build mathematical models to describe the relationships between the pre-layout and post-layout simulation results by the first few data samples of pre-layout and post-layout waveforms. The rest post-layout waveform can be predicted from the output of the system. Several examples demonstrate that the predicted waveforms provide more accurate information than the pre-layout waveforms and give the general trends of the post-layout waveforms. This method can be used to quickly explore the post-layout waveforms in the design process without time-consuming simulations.

TABLE II
NONLINEAR MODEL PREDICTION INFORMATION OF RING OSCILLATOR AND PLL

Circuits	Model type	Fit-level of validation (%)	Fit-level of prediction (%)	Model calibration time(s)	Prediction time (s)
ring-oscil	HM[a]	91.07	78.95	3.482	0.181
PLL	N-ARX[b]	89.85	73.50	1.358	1.819

[a] Hammerstein-Wiener Model
[b] Nonlinear ARX Model

ACKNOWLEDGMENT

This research is supported partly by National Natural Science Foundation of China (NSFC) research project 61125401, 61376040, 61228401, 61474026 and 91330201, partly by the National Basic Research Program of China under the grant 2011CB309701, partly by the National Major Science and Technology Special Project of China (2011ZX01035-001-001-003, 2014ZX02301002-002), partly by Shanghai Science and Technology Committee project 13XD1401100, partly by Chen Guang project supported by Shanghai Municipal Education Commission and Shanghai Education Development Foundation.

REFERENCES

[1] Kevin J Kerns and Andrew T Yang. Stable and efficient reduction of large, multiport rc networks by pole analysis via congruence transformations. *IEEE Transactions on Computer-Aided Design of Integrated Circuits and Systems*, 16(7):734–744, 1997.

[2] Bernard N Sheehan. TICER: Realizable reduction of extracted RC circuits. In *Proceedings of the 1999 IEEE/ACM international conference on Computer-aided design*, pages 200–203, 1999.

[3] A. Odabasioglu, M. Celik, and L. Pileggi. PRIMA: Passive reduced-order interconnect macromodeling algorithm. *IEEE Transactions on Computer-Aided Design of Integrated Circuits and Systems*, 17(8):645–654, Aug. 1998.

[4] R. Freund. SPRIM: Structure-preserving reduced-order interconnect macromodeling. In *Proceedings of IEEE/ACM International Conference on Computer-Aided Design*, pages 80–87, Nov. 2004.

[5] Chenjie Gu, Eli Chiprout, and Xin Li. Efficient moment estimation with extremely small sample size via bayesian inference for analog/mixed-signal validation. In *Proceedings of the 50th Annual Design Automation Conference*, page 65, 2013.

[6] Lennart Ljung. *System identification*. Wiley Online Library, 1999.

[7] Wouter Favoreel, Bart De Moor, and Peter Van Overschee. Subspace state space system identification for industrial processes. *Journal of Process Control*, 10(2):149–155, 2000.

[8] Shinji Ichikawa, Mutuwo Tomita, Shinji Doki, and Shigeru Okuma. Sensorless control of permanent-magnet synchronous motors using online parameter identification based on system identification theory. *IEEE Transactions on Industrial Electronics*, 53(2):363–372, 2006.

[9] Artificial neural network based system identification and model predictive control of a flotation column. *Journal of Process Control*, 19(6):991 – 999, 2009.

[10] Karel J Keesman. *System identification: an introduction*. Springer, 2011.

[11] Mathworks. Identifying Nonlinear ARX Model. http: //www.mathworks.com/help/, 2014.

[12] Feng Ding and Tongwen Chen. Identification of hammerstein nonlinear ARMAX systems. *Automatica*, 41(9):1479–1489, 2005.

[13] Mathworks. Compare outputs with measured data. http://www.mathworks.com/help/, 2013.